Electrochimica Acta 299 (2019) 762–771

Contents lists available at ScienceDirect

Electrochimica Acta

journal homepage: www.elsevier.com/locate/electacta

Investigation on acid functionalization of double-walled carbon nanotubes of different lengths on the development of amperometric sensors

Ana P. Lima [a], Ariadne C. Catto [b], Elson Longo [c], Edson Nossol [a], Eduardo M. Richter [a], Rodrigo A.A. Munoz [a, *]

[a] Institute of Chemistry, Federal University of Uberlândia, Av. João Naves de Ávila, 2121, Uberlândia, MG, Brazil
[b] Department of Physics, Federal University of São Carlos, 13565-905, São Carlos, SP, Brazil
[c] LIEC, Department of Chemistry, Federal University of São Carlos, 13565-905, São Carlos, SP, Brazil

ARTICLE INFO

Article history:
Received 17 October 2018
Accepted 8 January 2019
Available online 9 January 2019

Keywords:
Carbon
Catechol
Dopamine
Surface area
Phenolic compounds

ABSTRACT

Double-walled carbon nanotubes (DWCNTs) of different length were submitted to acid functionalization and investigated as chemical modifiers on glassy-carbon electrode (GCE) for the sensing of dopamine and catechol. Acid functionalization introduced oxygenated groups and defects on the structure of DWCNTs, as detected by infrared, Raman and X-ray photoelectron spectroscopy. However, cyclic voltammetric experiments showed higher current responses on non-functionalized (NF) DWCNTs. The decrease in response was stronger for shorter length nanotubes (S-DWCNT) modified GCE, which was attributed to the reduction of electroactive area of functionalized nanotubes after acid treatment with HNO_3/H_2SO_4. Brunauer-Emmett-Teller (BET) analyses confirmed the decrease in surface area of functionalized (F) DWCNTs, especially on F–S-DWCNT. Amperometric measurements also showed decrease in sensitivity and higher detection limit values on the F–S-DWCNT, which is also due to the decrease in electroactive area. As conclusion, DWCNT is a potential carbon-based material to the development of highly sensitive amperometric sensors and acid functionalization is not likely required due to the higher surface area provided by modification with the untreated material.

1. Introduction

The use of carbon nanostructures to provide the modification of surfaces has been intensively investigated in the development of electrochemical sensors. Carbon nanotubes (CNTs) are one of the major carbonaceous nanomaterials investigated and applied for this purpose [1–4]. The reason to select such a chemical modifier is related to the claimed electrocatalytic activity of CNTs, which is mainly attributed to defects located along the CNT structure [5,6]; however, additional factors may contribute, such as metallic impurities originating from their production [7] and change of the mass transport regime to thin-layer diffusion [8,9].

Most investigations found in the literature are devoted to multi-walled carbon nanotubes (MWCNTs) or single-walled carbon nanotubes (SWCNTs) while few reports demonstrating the use of double-walled carbon nanotubes (DWCNTs) can be found. Pumera [10] presented the first application of DWCNTs towards the detection of NADH with improved performance in comparison with SWCNTs. The insertion of DWCNTs into carbon paste electrodes was presented for the simultaneous determination of epinephrine, uric acid and folic acid [11], and ascorbic acid, dopamine and uric acid [12] as well as for the electrochemical reduction of oxygen [13]. Ferrocene encapsulated inside DWCNTs was proposed as an improved sensor for dopamine detection in the presence of excess of ascorbic acid [14]. DWCNTs have been proposed as a platform for biosensors and immunosensors [15,16] and combined with graphene oxide to provide a more sensitive electrochemical sensor to nitrite [17]. The work by Pumera [10] demonstrated that DWCNTs functionalized with concentrated nitric acid (to generate carboxylic groups) provided improved electrochemical response for the oxidation of NADH. Other previous works did not evaluate the effect of acid functionalization on the structure of DWCNTs. Moreover, to our knowledge there are no reports aimed to investigate the effect of sizes of DWCNTs on the electrochemistry of different

* Corresponding author.
E-mail address: munoz@ufu.br (R.A.A. Munoz).

https://doi.org/10.1016/j.electacta.2019.01.042
0013-4686/

electroactive compounds.

In this work, we investigate the application of DWCNTs of different dimensions and submitted to acid functionalization in the development of amperometric sensors for model catechol compounds, dopamine and catechol. DWCNTs were characterized by Raman and infrared spectroscopies, scanning electron microscopy (SEM), X-ray photoelectron spectroscopy (XPS), Brunauer-Emmett-Teller (BET) and cyclic voltammetry, and the performance of the respective amperometric sensors were compared using a batch-injection analysis system. The determination of catechol compounds, such as dopamine and catechol, is relevant for the analysis of biological fluids, pharmaceutical samples, natural water samples [18,19] and for this reason these compounds were selected for this investigation.

2. Experimental

2.1. Materials

Two types of double-walled carbon nanotubes were used in this work, the first one named as DWCNT (D x L: 3.5 nm × 1–10 μm, 90%) and a shorter one (D x L: 3.5 nm × 3 μm, 95%) named as S-DWCNT, both obtained from Sigma Aldrich (Milwaukee, WI, USA). Catechol (<99%) and dopamine (<99%) were obtained from Acros (New Jersey, USA), Sigma Aldrich (St. Louis, USA), respectively. The Britton-Robinson (BR) buffer solution was composed by a mixture of 0.1 mol L^{-1} acetic acid (99.7%), boric acid (PA), and phosphoric acid (85%) were obtained from Synth (Diadema, Brazil), QM (Cotia, Brazil) and Reagen (Rio de Janeiro, Brazil), respectively, and its different pH values were adjusted with sodium hydroxide from Dinâmica (Diadema, Brazil). Perchloric acid (70% v/v) from Reagen (Rio de Janeiro, Brazil) was used to prepare the supporting electrolyte. Hexaammine-ruthenium(III) chloride was purchased from Sigma Aldrich (Milwaukee, WI, USA). Deionized water with a resistivity of 18.2 MΩ cm obtained from a Milli Q water purification system (Millipore, Bedford, MA, USA) was used for preparing all aqueous solutions. All stock solutions of the analytes were prepared just before the experiments by dilution in 0.1 mol L^{-1} $HClO_4$.

2.2. Instrumentation

The electrochemical measurements were all performed using a PGSTAT128 N controlled by NOVA 1.11 software, responsible for the acquisition and processing of data. It was used an electrochemical cell with three distinct electrodes. A platinum wire, used as auxiliary electrode or counter electrode; a miniaturized Ag/AgCl/KCl saturated electrode as reference [20] and a glassy carbon electrode (GCE) (Ø = 1.6 mm diameter acquired from Basi - West Lafayette, USA), as working electrode.

2.3. Electrochemical measurements

Cyclic voltammetric experiments were carried out using a 10 mL glass electrochemical cell containing the three-electrode system. Amperometric measurements were performed in a labmade batch-injection analysis (BIA) cell developed by our research group [21]. This technique requires an injector, an electronic micropipette in the case of this work, which injects controlled aliquots of solution over the working electrode placed at the bottom of the cell, in a "wall jet" configuration. The BIA electrochemical cell is constituted by a cylindrical vessel filled with 200 mL of supporting electrolyte with a top cover that fits reference and counter electrodes beside the entrance of the micropipette tip. The motorized electronic pipette (Eppendorf Multipette® stream) connected with the Multipette® Combitip® tip was maintained at fixed distance of 2 mm from the surface of the working electrode and was programmed to inject 100 μL under a dispensing rate of 153 μL s^{-1}. The BIA cell representation is shown in Fig. 1. These conditions were optimized in previous works to provide fast analytical responses [22].

All electrochemical measurements were performed at room temperature and in the presence of dissolved oxygen.

2.4. Functionalization of DWCNTs

An amount of 500 mg of raw DWCNTs was first treated with a 3:1 (v/v) mixture of concentrated H_2SO_4 and HNO_3 acids (550 mL). This mixture was then sonicated for 3 h at 40 °C in an ultrasonic bath to introduce oxygenated groups on the DWCNT surface. After cooling to room temperature, the functionalized DWCNTs were added dropwise to 1000 mL of cold deionized water and then vacuum-filtered through a filter paper with pore size of 0.05 mm. The filtrate was then washed with deionized water continuously until the pH became neutral. The sample was then dried in a vacuum oven at 80 °C for 8 h [23].

2.5. Electrode modification with the DWCNTs

The cleaning of the working electrode surface was executed mechanically before and after the analysis on a felt-polishing pad using an alumina powder suspension (0.3 μm) and rinsing copiously with deionized water followed by sonication in water/ethanol solution. The DWCNT dispersion was prepared by adding 0.5 mg mL^{-1} in dimethylformamide (DMF), the dispersion of the S-DWCNT was prepared by adding 1.0 mg mL^{-1} in DMF. The dispersion was sonicated using ultrasonic bath for 10 min and high-frequency sonication tip for 20 min (amplitude: 30% with a pulse of 5 to 2 s). The dispersions were selected based on the optimization study that evaluated the ideal dispersion for each DWCNT. A dispersion of 10 μL was placed on the surface of the bare GCE and the electrode was then heated for 30 min at 50 °C, resulting in the modified electrode.

2.6. Characterization of DWCNTs

The infrared spectroscopy analyses were performed using an equipment Spectrum two model of Perkin Elmer, with ATR crystal. Samples were evaluated in their powder form, without the need for any previous treatment. Eight scans were carried out in the range of 4000 to 600 cm^{-1} at a resolution of 4 cm^{-1}.

To obtain the Raman spectra of the non-functionalized and functionalized DWCNTs, a Renishaw spectrophotometer coupled to an optical microscope with a spatial resolution of 1 μm was used. A He–Ne laser (632.8 nm) was used with 2 mW incidence power. Samples were used in their powder form, in the region between 130 and 3000 cm^{-1} and accumulation time of 20 s.

The scanning electron microscopic (SEM) images of DWCNT in high resolution were performed using a Mira FEG-SEM (TESCAN) at 10 kV. For the analysis of the GCE surfaces modified with DWCNTs was used a Vega 3 LMU (TESCAN, Brno-Kohoutovice, Czech Republic) operated at 20 kV.

X-ray photoelectron spectroscopy (XPS) analyses were performed on a Scienta Omicron, model ESCA + spectrometer using monochromatic AlKα (1486.6 eV) radiation. Peak decomposition was performed using a Gaussian-Lorentzian line shape with a Shirley nonlinear sigmoid-type baseline. The binding energies were corrected for charging effects by assigning a value of 284.8 eV to the adventitious C 1s line. The data were analyzed using CasaXPS software (Casa Software Ltd., U.K.).

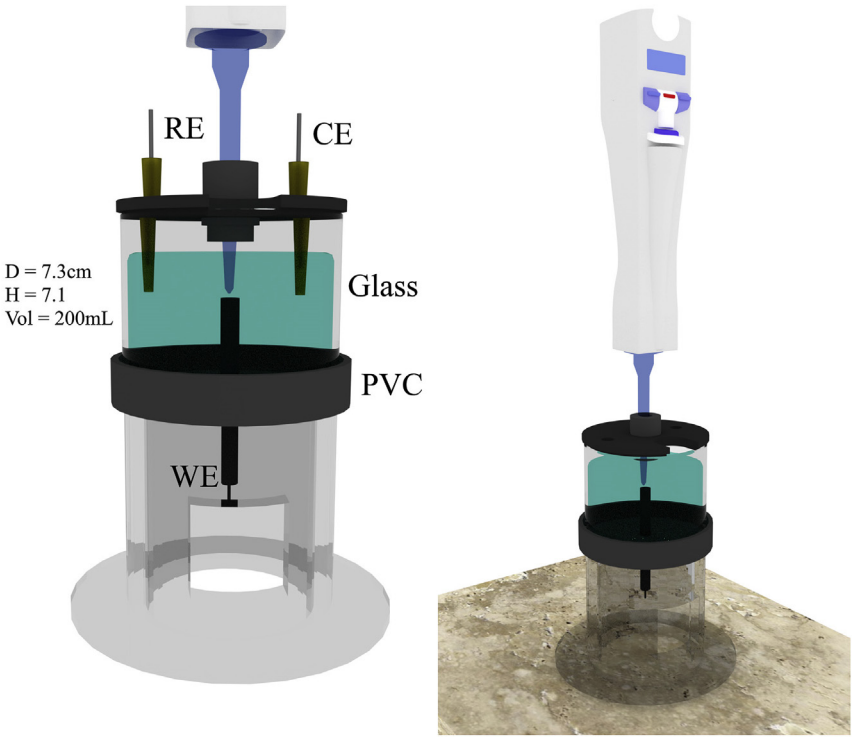

Fig. 1. (A) Representation of the 'wall jet' electrochemical cell for BIA system; (B) electronic pipette positioned in the BIA cell, conformation used for amperometric measurements.

The N_2 adsorption-desorption isotherms were performed at −196 °C using a NOVAtouch surface area analyzer with QuantachromeTouchWin software (version 1.1.). Specific surface area was calculated using the Brunauer, Emmett and Teller method (BET) [24,25]. All powders samples were degassed in vacuum at 200 °C during 4 h for the surface area determination.

3. Results and discussion

3.1. Characterization of DWCNTs

Both DWCNT and S-DWCNT powders were characterized by different techniques before and after acid functionalization in order to investigate surface modification due to the acid treatment. The infrared spectra for DWCNT and S-DWCNT are presented in Fig. 2.

DWCNT and S-DWCNT present coincident bands at 2901 and 2836 cm^{-1}, equivalent to the symmetric and asymmetric stretching modes of C–H groups [26], respectively. The region between 1520 and 1433 cm^{-1} for both DWCNTs corresponds to the deformation of the C–H bond [27]. Functionalized DWCNT and S-DWCNT present bands in the range between 3700 and 3000 cm^{-1} that indicate the presence of carboxylic and hydroxyl groups resulting from the axial deformation of the –OH bond [26]. The width of these bands indicates that different groups containing hydroxyls, such as carboxylic, alcoholic or phenolic groups, are probably present [28]. In the region between 2900 and 2836 cm^{-1}, increase in the intensity

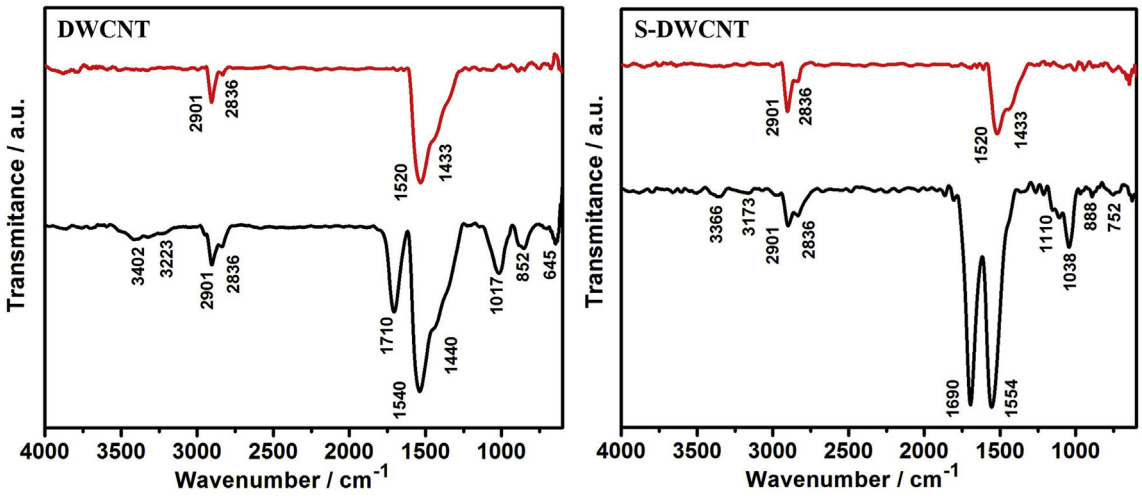

Fig. 2. Infrared spectra obtained using ATR mode for (NF) non-functionalized (—) and (F) functionalized (╍) DWCNT and S-DWCNT.

of the bands occurs, which corresponds to the symmetrical and asymmetric stretching of C–H groups [29]. Functionalized DWCNT and S-DWCNT exhibit intense bands in the region between 1850 and 1650 cm^{-1}, corresponding to the stretching of C=O bonds [30,31]. The bands in the region between 1540 and 1565 cm^{-1} are attributed to the stretching of C=C bonds and their higher intensity is mainly due to the induction of dipole moments by creating defects in the walls of nanotubes [26]. Functionalized DWCNT and S-DWCNT also present bands in the region between 1300 and 900 cm^{-1} corresponding to the stretching of the C–O bond [32,33]. Bands in the region between 900 and 600 cm^{-1} are typically from C=C bonds of CNTs [27]. Therefore, it is clear from the analysis of spectroscopic data that both DWCNT and S-DWCNT were functionalized with oxygenated groups after the acid treatment.

Fig. 3 presents Raman spectra for DWCNT and S-DWCNT. The D band is formed by vibrational stretching modes of C–C that become active by loss of symmetry when there are defects in the hexagonal network of graphene [34]. Therefore, the D band is induced by structural disorder, such as vacancies, heteroatoms, pentagonal-heptagon pairs, junctions, folds, sp^2 to sp^3 hybridization, which may also be present in any graphitic material [35,36]. The G band is associated to the vibration mode in graphitic materials (sp^2 hybridization), in which two carbon atoms in the graphene sheet move tangentially against each other [37]. The 2D band corresponds to the D band overtones and is related to the changes in the electronic structure of the nanotubes and to the two-dimensional order of graphene [38].

DWCNT and S-DWCNT present similar Raman spectra. The change in the intensity of the bands proves that the functionalization occurred effectively. Functionalization typically causes an increase in the D band and consequently the I_D/I_G ratio increases when comparing the spectra for the functionalized and non-functionalized CNTs, which is correlated with the degree of CNT disorder and with the presence of more structural defects. The I_D/I_G ratios for non-functionalized DWCNT and S-DWCNT were 0.33 and 0.44, respectively, while for functionalized DWCNT and S-DWCNT were 0.50 and 0.63, respectively. The I_D/I_G values are higher for the functionalized DWCNTs probably due to more structural defects in their CNT structures.

XPS data were used to examine the chemical states of the samples. Figs. S1 and S2 present the XPS analyses of DWCNT and S-DWCNT before and after the functionalization process. The high-resolution C1s spectra (Fig. S1) presented five components, labeled as C1s(1), C1s(2), C1s(3), C1s(4) and C1s(5). The component at approximately 285.6 eV (C1s (2)), and the two subsequent peaks at 286.9 eV, 288.5 eV were assigned to different oxygen-containing functional groups, as C–O, C=O, –COO respectively [39]. The relative concentration of each component to total area calculated based on the deconvoluted XPS C1s spectra was summarized in Table 1. It can be seen that the amount of components C1s(3) and C1s(4) which are assigned to carbon–oxygen double bonds in carboxylic acids, carboxylic anhydrides and esters (–COO) increased after functionalization process. The high-resolution O1s spectra were also measured and deconvoluted into two components, as illustrated in Fig. S2. The lower energy peak at 531.7 eV was attributed to the oxygen doubly bound to carbon (i.e., O=C). The second component at approximately 533.0 eV was assigned to oxygen singly bound to carbon (i.e., O–C). Indeed, according to the amount of ratio of the peak areas obtained from XPS analysis (Table 1), an increase in the first component was observed for the functionalized CNTs. Thus XPS results confirm the functionalization of CNTs with oxygen-containing functional groups after acid treatment, as related in infrared studies.

In order to investigate the effect of acid treatment in the surface area of the carbonaceous materials, BET analyses were performed and the results are summarized in Table 2. It is clear that treatment using the mixture of HNO_3 and H_2SO_4 acids decreases the surface area of both types of CNTs. The introduction of functional groups and intercalated acid molecules acts blocking the entry of the

Table 1
XPS of C1s and O1s peaks area of components to total area.

	C 1s (3) 287.3 eV	C 1s (4) 288.7 eV	O=C 531.7 eV
NF – S-DWCNT	3.4%	2.3%	11.2%
F – S-DWCNT	3.9%	10.8%	18.6%
NF - DWCNT	5.9%	1.4%	5.0%
F - DWCNT	5.9%	4.1%	8.0%

Table 2
Specific surface area of DWCNTs obtained by BET analyses.

	Surface area/$m^2\ g^{-1}$
NF–S-DWCNT	331.7
F–S-DWCNT	194.5
NF-DWCNT	411.0
F-DWCNT	378.3

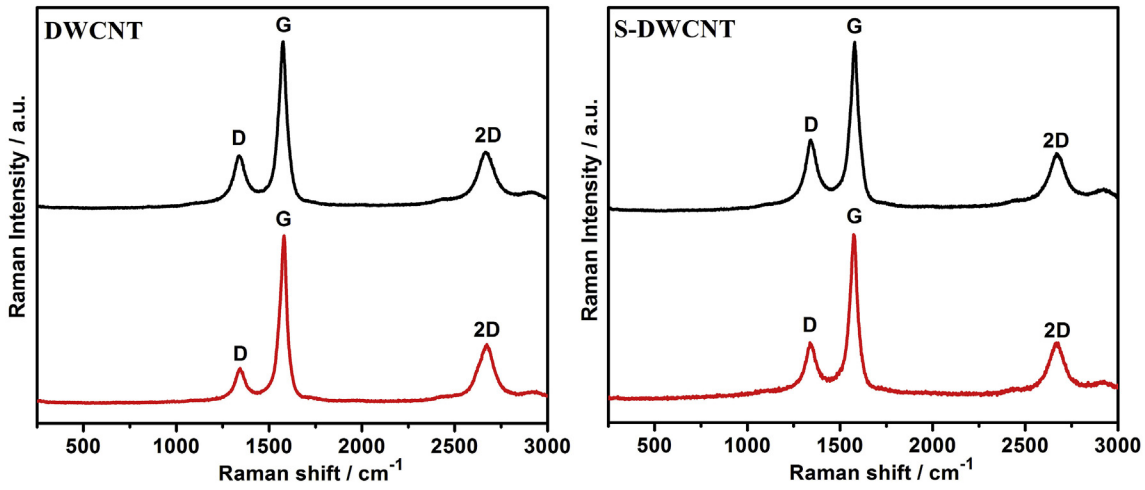

Fig. 3. Raman spectra for non-functionalized (—) and functionalized (▪) DWCNT and S-DWCNT.

adsorbing gas, resulting in decrease in surface area [40]. The decrease in surface area was more intense in the NF–S-DWCNTs due to the smaller dimension of this DWCNT and consequently the acid attack was more effective. On other hand, the unexpected lower surface area of NF–S-DWCNT in comparison with NF-DWCNT (before acid treatment) may be explained by agglomeration of the smaller NF–S-DWCNT particles.

3.2. Electrochemical measurements of model catechol compounds

Dopamine and catechol were selected as model analytes to compare the performance of DWCNT-modified electrodes with previous works. Fig. S3 shows cyclic voltammetric experiments for both compounds in different electrolyte solutions, including Britton-Robinson buffer solution (pH 2.0, 4.0 and 6.0) and 0.1 mol L^{-1} $HClO_4$. Slightly higher current responses were obtained in 0.1 mol L^{-1} $HClO_4$ which was selected for further experiments in this work. Cyclic voltammetric measurements of these compounds in 0.1 mol L^{-1} $HClO_4$ using non-functionalized and functionalized S-DWCNT and DWCNT are presented in Fig. 4.

The first evidence observed from the cyclic voltammetric experiments is the facilitated electron transfer observed on all

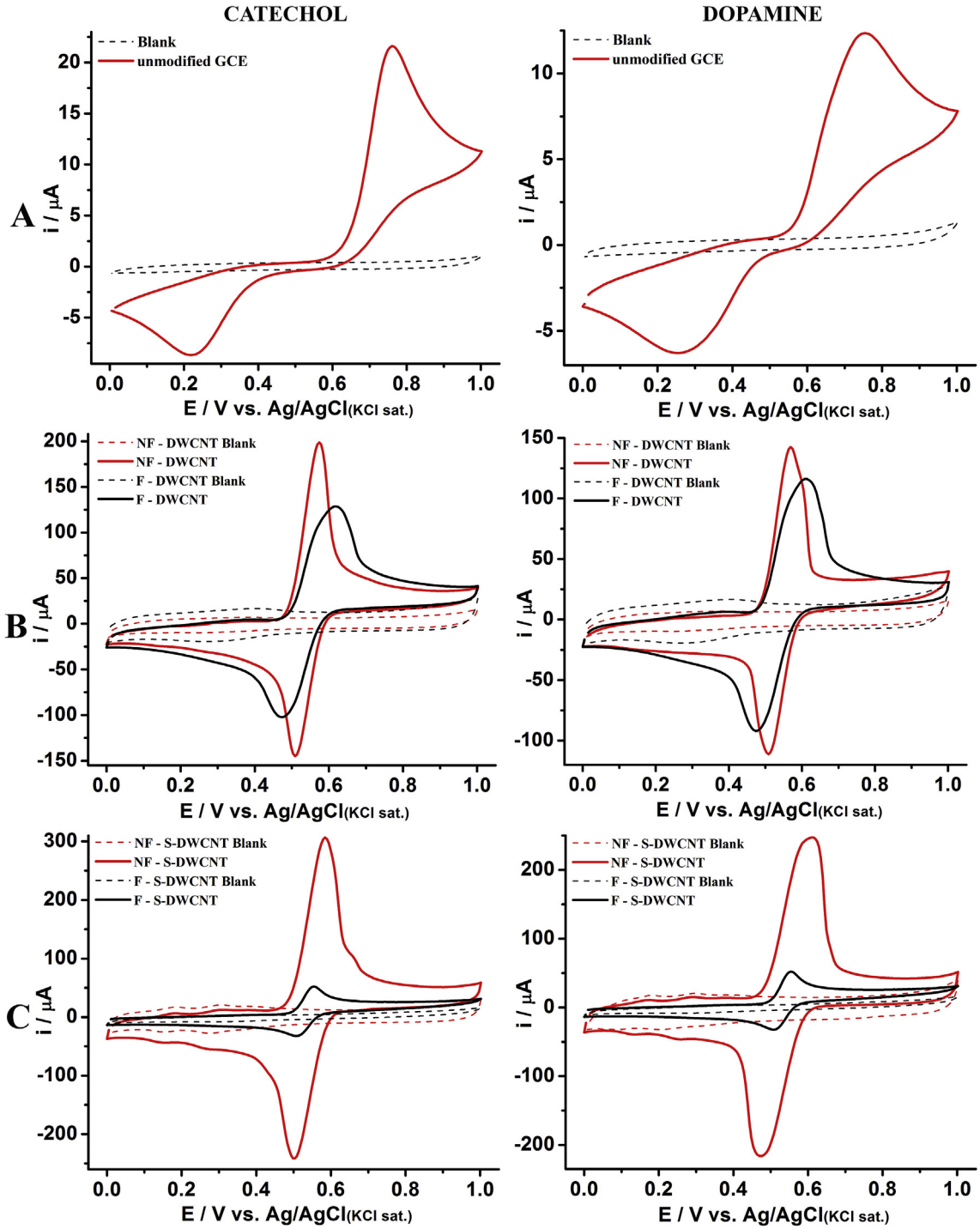

Fig. 4. Cyclic voltammograms of 1.0 mmol L^{-1} for CA and DA in 0.1 mol L^{-1} $HClO_4$ solution. **A**: Unmodified GCE (—); **B:** DWCNT, non-functionalized (NF) (—) and functionalized (F) (-); and **C**: S-DWCNT, (NF) (—) and (F) (-). Scan rate: 50 mV s^{-1}, potential scanned from 0 to +1.0 V. Dashed lines correspond to blanks.

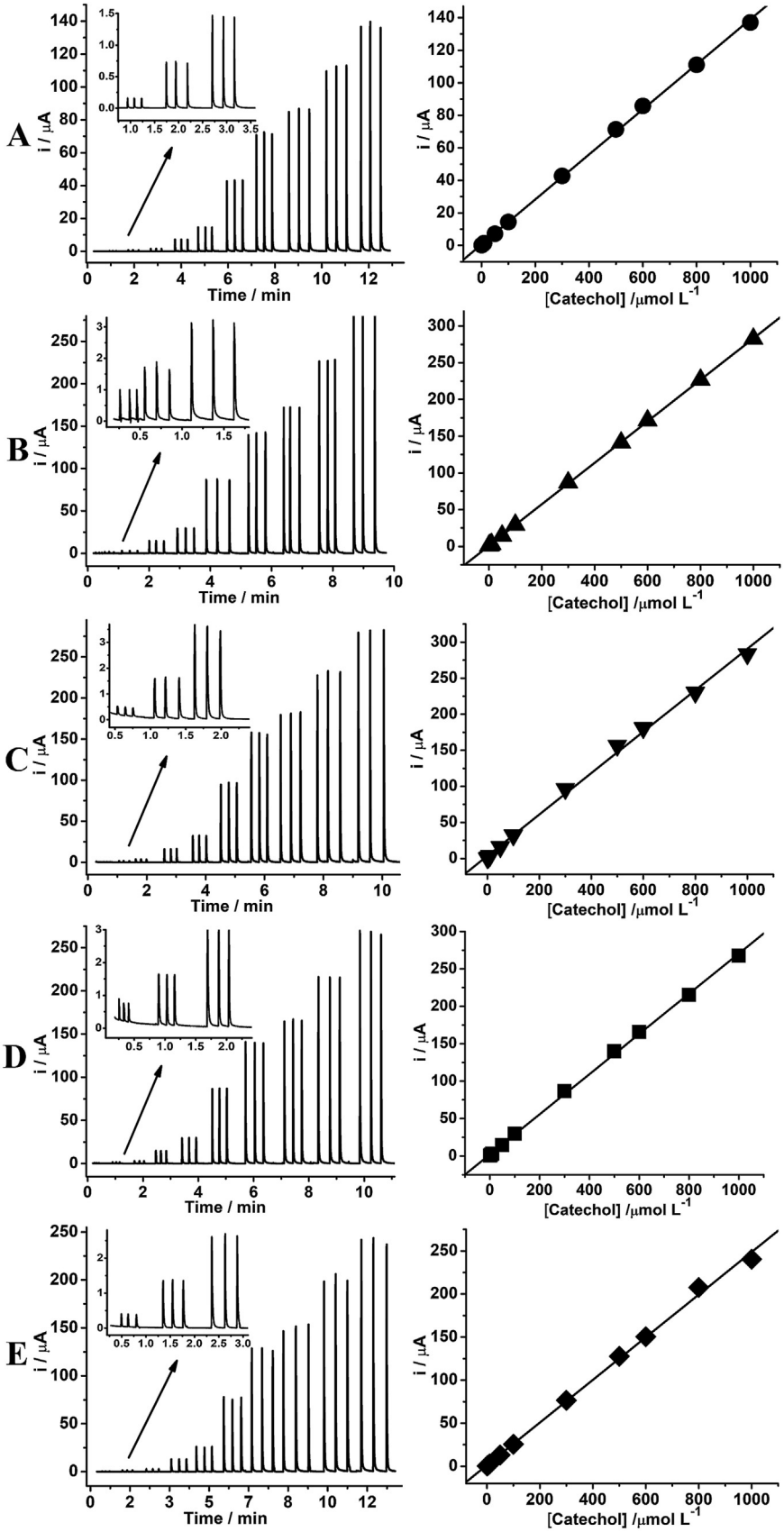

Fig. 5. Amperometric responses obtained in BIA using unmodified GCE (A), NF– DWCNT (B), F-DWCNT (C), NF–S-DWCNT (D), and F–S-DWCNT (E) for triplicate injections of CA standard solutions 1, 5, 10, 50, 100, 300, 500, 600, 800 and 1000 μmol L^{-1} in 0.1 mol L^{-1} $HClO_4$. On the right side, the respective analytical curves highlighting the linear working ranges. Working potential: +0.7 V, injected volume: 100 μL; dispensing rate: 153 μL s^{-1}.

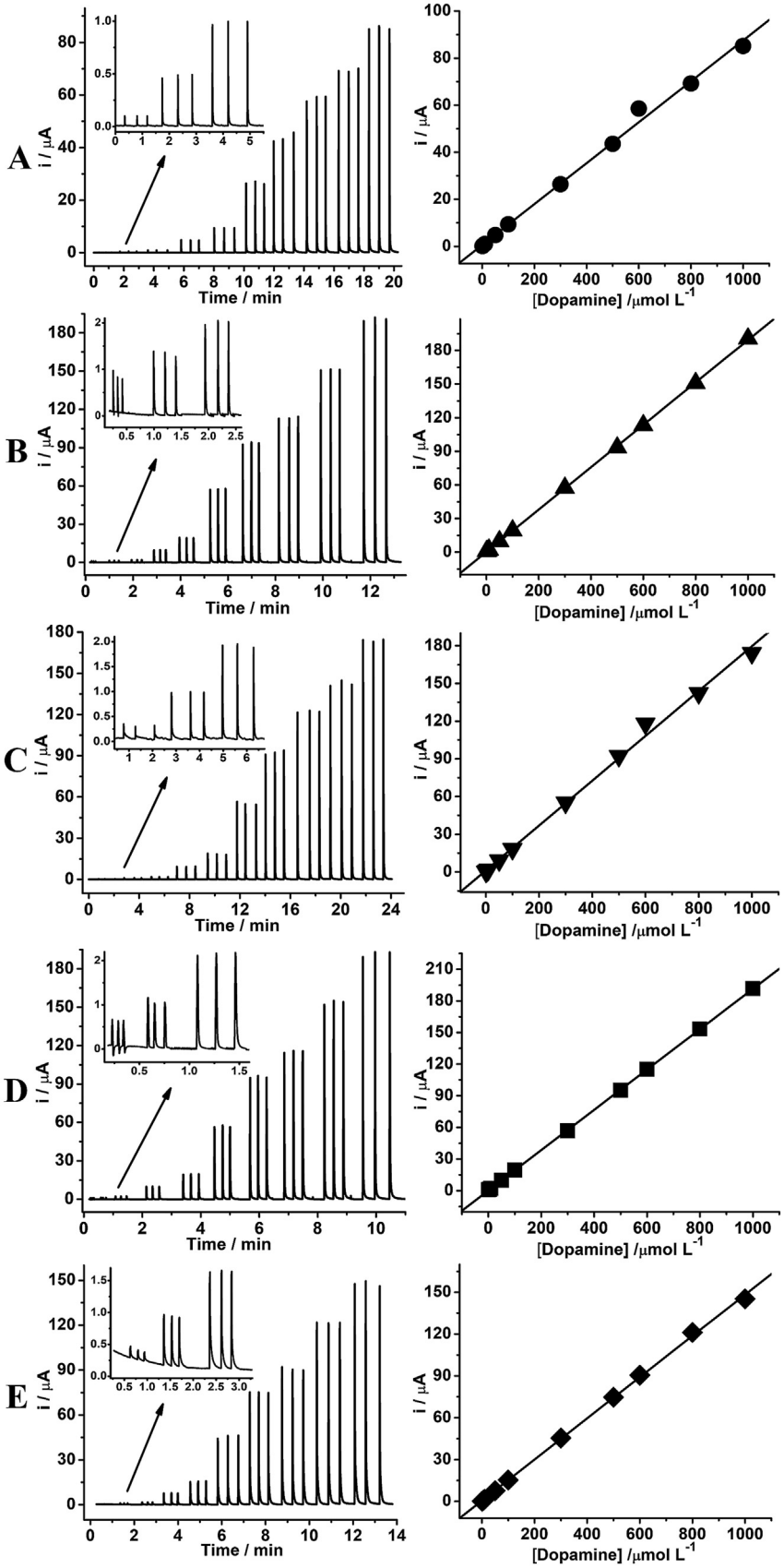

Fig. 6. Amperometric responses obtained in BIA using unmodified GCE (A), NF– DWCNT (B), F-DWCNT (C), NF–S-DWCNT (D), and F–S-DWCNT (E) for triplicate injections of DA standard solutions 1, 5, 10, 50, 100, 300, 500, 600, 800 e 1000 μmol L^{-1} in 0.1 mol L^{-1} $HClO_4$. On the right side, the respective analytical curves highlighting the linear working ranges. Working potential: +0.7 V, injected volume: 100 μL; dispensing rate: 153 μL s^{-1}.

modified electrodes with DWCNT in comparison with the unmodified GCE as shown by the reduced peak-to-peak separation (ΔE) values. ΔE values for the electrochemical oxidation of catechol and dopamine on unmodified GCE were around 500 mV, while this value was not higher than 200 mV for the voltammograms performed using the modified surfaces.

The acid functionalization of DWCNT affected the cyclic voltammetry of both analytes, especially when the electrode surface was modified with S-DWCNT. IR, XPS and Raman spectroscopy data in combination with SEM images (Fig. S4) evidenced the successful functionalization of DWCNTs by insertion of oxygenated groups and higher density of defects on the nanotubes maintaining their morphological properties. Smaller length DWCNTs are more affected by the acid treatment, which corroborated with XPS results. Previous works have demonstrated that acid functionalization of CNTs with sulfonitric acid mixture leads to decrease in the electroactive area [41–44]. Therefore, the smaller currents especially obtained on the functionalized S-DWCNT-modified GCE may be a result from the decrease in electroactive area, which was more intense on the S-DWCNT due to its reduced length. These results are also corroborated by BET analysis displayed in Table 2, in which S-DWCNTs were more affected by acid treatment compared with DWCNTs. Higher background currents (blank experiments in Fig. 4) also indicate the higher electroactive area of non-functionalized S-DWCNT in comparison with functionalized DWCNT. Blank experiments obtained on NF–S-DWCNTs reveal slight current signals between +0.2 and + 0.3 V that may be a contribution of residual metallic impurities on NF–S-DWCNTs which are removed after acid functionalization as described in the literature [44].

The electroactive area of the modified electrodes was estimated using the Randles-Sevick equation applied to the cyclic voltammetric data for 1 mmol L^{-1} hexaammine-ruthenium(III) chloride in 0.1 mol L^{-1} KCl in the range of 10 and 100 mV s^{-1}. The values obtained from the electroactive area were 17.97 mm^2 (NF-DWCNT), 14.88 mm^2 (F-DWCNT), 19.78 mm^2 (NF–S-DWCNT), 12.70 mm^2 (F–S-DWCNT). These data corroborate with BET analyses, which showed decrease in surface area after acid functionalization and that S-DWCNTs were more affected by the acid treatment.

Next, the effect of scan rate (10–100 mV s^{-1}) of cyclic voltammetry was evaluated to investigate the electrode kinetics in all modified surfaces for both analytes. The plots of log *Ip* *vs.* log *v* were linear with slope values around 0.5 in all modified surfaces, which indicates a diffusion-controlled regime mass transfer (see Fig. S5 and Table S1). Nevertheless, voltammetric experiments performed in blank solution immediately after a voltammetric experiment in the presence of analyte showed current responses due to the entrapment of the phenolic compounds within the DWCNT film, demonstrating that adsorption-controlled processes also occur (see Fig. S6). This result was also observed in previous works for electrodes modified with CNT [8,9,44–46], and it may contribute to the variation of current observed in the cyclic voltammetric experiments.

Amperometric measurements were performed with the aid of BIA. First, the applied potential for further amperometric measurements were selected based on the plot of current *vs.* applied potential. The average current for triplicate injections of the analyte solution was obtained using the amperometric technique and this experiment was repeated for different applied potentials. The less positive applied potential which produced higher current responses under hydrodynamic conditions was +0.7 V on unmodified and modified electrodes, and thus was selected for further amperometric detection of dopamine and catechol. Additional parameters to be optimized were related to the BIA technique, such as injection volume and rate. The values, which generated higher current responses, were 100 μL and 153 μL s^{-1} within the ranges of 10–200 μL and 28–257 μL s^{-1}, respectively. Next, calibration curves were obtained under these optimized conditions for dopamine and catechol on unmodified and modified GCE with non-functionalized and functionalized DWCNTs. Figs. 5 and 6 presents all amperometric measurements corresponding to the calibration curves, and Table 3 summarizes the analytical characteristics calculated from the data of Figs. 5 and 6.

Analytical curves presented wide linear range with adequate correlation coefficients. Slope values followed similar trend observed in the cyclic voltammetric experiments, in which lower currents were observed for the functionalized S-DWCNT-modified GCE. Detection and quantification limits were improved when the modified electrode was employed and higher difference of slope values was observed for the functionalized S-DWCNT-modified GCE. Therefore, the analytical sensitivity obtained using amperometric detection is likely to be proportional to the electroactive area of the modified electrode, in agreement with cyclic voltammetry and BET experiments.

Hence, the results show that the effect of acid functionalization of DWCNTs on the generation of more oxygenated groups and defects on the structure was not relevant on the construction of amperometric sensors for phenolic compounds, considering the use of DWCNTs. The values of detection limits and linear concentration range obtained for catechol and dopamine are compared with data from the literature as presented in Table 4. The values of both analytical parameters obtained using DWCNTs indicate improved performance in comparison with most of the works listed in this table. Additional information on DWCNT-modified electrodes was the high precision using the different DWCNTs (respective amperometric recordings are shown in Fig. S7); repeatability study showed relative standard deviation values lower than 1.4% (n = 10). The inter-electrode reproducibility studies were performed in triplicate for all DWCNTs and the relative standard deviations obtained were lower than 4.4% (Table S1).

Comparing the analytical sensitivity of such modified electrodes with GCE modified with MWCNTs using the same BIA system (and GCE of similar geometric area), the sensitivity values (μA L $μmol^{-1}$) for the determination of CA and DA were similar, corresponding to, respectively, 0.301 and 0.259 on NF-MWCNT/GCE, 0.180 and 0.148 on F-MWCNT/GCE [44], 0.167 and 0.138 on MWCNT/GCE [48]. A previous study [44] also showed higher analytical sensitivity for the detection of catechol compounds when NF-MWCNTs were used instead of F-MWCNTs.

4. Conclusions

We have demonstrated the potential application of DWCNTs to

Table 3
Analytical characteristics calculated from calibration curves (1–1000 μmol L^{-1}) for catechol and dopamine obtained on unmodified GCE and after modification with NF-DWCNT, F-DWCNT, NF– S-DWCNT, and F–S-DWCNT.

	Electrodes	Slope μA L $μmol^{-1}$	R	LOD μmol L^{-1}
Catechol	GCE	0.1385 ± 0.0011	0.9997	0.87
	NF - DWCNT	0.2824 ± 0.0007	0.9999	0.046
	F - DWCNT	0.2874 ± 0.0051	0.9987	0.014
	NF – S-DWCNT	0.2685 ± 0.0024	0.9996	0.024
	F – S-DWCNT	0.2478 ± 0.0040	0.9989	0.072
Dopamine	GCE	0.0870 ± 0.0021	0.9977	1.03
	NF - DWCNT	0.1891 ± 0.0007	0.9999	0.058
	F - DWCNT	0.1784 ± 0.0037	0.9982	0.049
	NF – S-DWCNT	0.1911 ± 0.0004	0.9999	0.037
	F – S-DWCNT	0.1478 ± 0.0014	0.9996	0.174

The limits of detection (LOD) were calculated according to IUPAC, where LOD = 3sB/S (sB is the standard deviation of the intercept and S is the slope of the calibration curve) [47].

Table 4
Comparison of the different analytical results obtained in the determination of CA and DA using DWCNT/GCE and S-DWCNT/GCE, non-functionalized (NF) and functionalized (F).

Electrodes	Analyte	Technique	Linear range μmol L^{-1}	LD μmol L^{-1}	Reference
PDDA-G/GCE	CA	CV	1–400	0.2	[49]
GR - chitosan/GCE	CA	DPV	1–400	0.7	[50]
GR/GCE	CA	DPV	1–50	0.01	[51]
RGO-MWCNT/GCE	CA	CV and DPV	5.5–540	1.8	[52]
NiO/MWCNT/GCE	CA	DPV	7.4–56	0.015	[53]
MnPc/MWCNT/GCE	CA	CV and DPV	1–600	0.095 and 0.096	[54]
*MWCNT/GCE	CA	AMP	0.5–1000	0.170	[48]
NF - *MWCNT/GCE	CA	AMP	0.5–1000	0.06	[44]
NF– DWCNT/GCE	CA	AMP	1–1000	0.046	This work
F– DWCNT/GCE	CA	AMP	1–1000	0.014	This work
NF – S-DWCNT/GCE	CA	AMP	1–1000	0.024	This work
F – S-DWCNT/GCE	CA	AMP	1–1000	0.072	This work
Fc-SWCNT/GCE	DA	CV and DPV	5–30	0.0500	[55]
MWCNT/GCE	DA	DPV	0.05–5	0.0110	[56]
MWCNT-EDAS-AuNPs/GCE	DA	CV and DPV	0.1–80	0.080	[57]
$[Co(phen)^3]^{2+}$/MWCNT/GCE	DA	AMP	5–453	1.760	[58]
CoNPs/MWCNT/GCE	DA	SWV	0.05–3.0	0.150	[59]
PMB/MWCNT/GCE	DA	CV	2.5–755	67	[60]
*MWCNT/GCE	DA	AMP	0.1–1000	0.030	[48]
NF - *MWCNT/GCE	DA	AMP	0.5–1000	0.040	[44]
NF - DWCNT/GCE	DA	AMP	1–1000	0.058	This work
F - DWCNT/GCE	DA	AMP	1–1000	0.049	This work
NF – S-DWCNT/GCE	DA	AMP	1–1000	0.037	This work
F – S-DWCNT/GCE	DA	AMP	1–1000	0.174	This work

PDDA-G - poly (diallyldimethylammonium chloride) - graphene; GR - graphene, RGO reduced graphene oxide; NiO - nickel oxide nanoparticles, MnPc - manganese phthalocyanine azo-macrocycle.; *MWCNT - multi walled carbon nanotube (dimension D x L: 6–9 nm x 5 μm); Fc- Ferrocene; EDAS - N-[3(trimethoxysilyl)propyl]ethylenediamine; AuNPs - Gold nanoparticles; Co(phen) - Cobalt phenanthroline; CoNPs - cobalt nanoparticle; PMB - poly(methylene blue); CV - cyclic voltammetry; DPV - Differential pulse voltammetry; AMP - amperometric detection; SWV - square wave voltammetry.

develop highly sensitive amperometric sensors to catechol and dopamine. Acid treatment of DWCNTs of different lengths was evaluated and IR, Raman, and XPS spectroscopy revealed the successful functionalization of the nanotube structure. However, the insertion of oxygenated groups as well as the increase in defects on the DWCNT structure did not provide improved electroanalytical performance of the modified electrodes as amperometric sensors. On the other hand, the changes of electroactive area due to acid functionalization measured by BET and cyclic voltammetric experiments presented a strong influence on the current responses. Cyclic voltammetry, XPS, and BET analyses indicated that smaller length DWCNTs were more affected by the acid functionalization which resulted in a more intense decrease in the electroactive area of the respective modified electrode. As a consequence, the amperometric sensitivity towards the detection of dopamine and catechol on the functionalized S-DWCNT-modified electrode was more reduced and is likely to be a result of decrease in the electroactive area. Therefore, the use of untreated DWCNT seems to be the best choice in the development of amperometric sensors.

Acknowledgement

The authors are grateful to CNPq (307271/2017-0, 307333/2014-0 and 481086/2012-9), FAPEMIG (PPM-00236-12), CAPES (23038.007073/2014–12) and FINEP for financial support and to the Multiuser Laboratory of Chemistry Institute at the Universidade Federal de Uberlândia for providing the equipment and technical support for experiments involving scanning electron microscopy. The authors would also like to thank Materials Chemistry Group at Federal University of Paraná for support in obtaining Raman data and FEG-SEM images and Prof. Valmor R. Mastelaro for XPS experiments.

Appendix A. Supplementary data

Supplementary data to this article can be found online at https://doi.org/10.1016/j.electacta.2019.01.042.

References

[1] G.G. Wildgoose, C.E. Banks, H.C. Leventis, R.G. Compton, Chemically modified carbon nanotubes for use in electroanalysis, Microchimica Acta 152 (2006) 187–214.
[2] L. Agui, P. Yanez-Sedeno, J.M. Pingarron, Role of carbon nanotubes in electroanalytical chemistry: a review, Anal. Chim. Acta 622 (2008) 11–47.
[3] I. Dumitrescu, P. Unwin, J.V. Macpherson, Electrochemistry at carbon nanotubes: perspective and issues, Chem. Commun. 45 (2009) 6886–6901.
[4] M. Pumera, Voltammetry of carbon nanotubes and graphenes: excitement, disappointment, and reality, Chem. Rec. 12 (2012) 201–213.
[5] C.E. Banks, R.R. Moore, T.J. Davies, R.G. Compton, Investigation of modified basal plane pyrolytic graphite electrodes: definitive evidence for the electrocatalytic properties of the ends of carbon nanotubes, Chem. Commun. 16 (2004) 1804–1805.
[6] C.E. Banks, T.J. Davies, G.G. Wildgoose, R.G. Compton, Electrocatalysis at graphite and carbon nanotube modified electrodes: edge-plane sites and tube ends are the reactive sites, Chem. Commun. 7 (2005) 829–841.
[7] C.E. Banks, A. Crossley, C. Salter, S.J. Wilkins, R.G. Compton, Carbon nanotubes contain metal impurities which are responsible for the "electrocatalysis" seen at some nanotube-modified electrodes, Angew. Chem. Int. Ed. 45 (2006) 2533–2537.
[8] M.J. Sims, N.V. Rees, E.J.F. Dickinson, R.G. Compton, Effects of thin-layer diffusion in the electrochemical detection of nicotine on basal plane pyrolytic graphite (BPPG) electrodes modified with layers of multi-walled carbon nanotubes (MWCNT-BPPG), Sensor. Actuator. B 144 (2010) 153–158.
[9] G.P. Keeley, M.E.G. Lyons, The effects of thin layer diffusion at glassy carbon electrodes modified with porous films of single-walled carbon nanotubes, Int. J. Electrochem. Sci. 4 (2009) 794–809.
[10] M. Pumera, Electrochemical properties of double wall carbon nanotube electrodes, Nanoscale Res. Lett. 2 (2007) 87–93.
[11] H. Beitollahi, M.M. Ardakani, B. Ganjipour, H. Naeimi, Novel 2,2'-[1,2-ethanediylbis(nitriloethylidyne)]-bis-hydroquinone double-wall carbon nanotube paste electrode for simultaneous determination of epinephrine, uric acid and folic acid, Biosens. Bioelectron. 24 (2008) 326–368.
[12] B. Xu, Q. Song, H. Wang, Simultaneous determination of ascorbic acid, dopamine, and uric acid based on double-walled carbon nanotubes/choline-

modified electrode, Anal. Methods 5 (2013) 2335–2342.
[13] I. Kruusenberg, L. Matisen, H. Jiang, M. Huuppola, K. Kontturi, K. Tammeveski, Electrochemical reduction of oxygen on double-walled carbon nanotube modified glassy carbon electrodes in acid and alkaline solutions, Electrochem. Commun. 12 (2010) 920–923.
[14] H. Cheng, Q. Qiu, Z. Chu, M. Li, Z. Shi, Investigation of the electrochemical behavior of dopamine at electrodes modified with ferrocene-filled double-walled carbon nanotubes, Electrochim. Acta 63 (2012) 83–88.
[15] U. Anik, S. Çevik, Double-walled carbon nanotube based carbon paste electrode as xanthine biosensor, Microchimica Acta 166 (2009) 209–213.
[16] I. Ojeda, M. Barrejon, L.M. Arellano, A. Gonzalez-Cortes, P. Yanez-Sedeno, F. Langa, J.M. Pingarron, Grafted-double walled carbon nanotubes as electrochemical platforms for immobilization of antibodies using a metallic-complex chelating polymer: application to the determination of adiponectin cytokine in serum, Biosens. Bioelectron. 74 (2015) 24–29.
[17] W. Liu, Y. Gu, G. Sun, K. Na, C. Li, L. Tang, Z. Zhang, M. Yang, Poly(-diallydimethylammonium chloride) functionalized graphene/double-walled carbon nanotube composite for amperometric determination of nitrite, Electroanalysis 28 (2016) 484–492.
[18] J.A. Ribeiro, P.M. Fernandes, C.M. Pereira, F. Silva, Electrochemical sensors and biosensors for determination of catecholamine neurotransmitters: a review, Talanta 160 (2016) 653–679.
[19] F.C. Vicentini, L.L. Garcia, L.C. Figueiredo-Filho, B.C. Janegitz, O. Fatibello-Filho, A biosensor based on gold nanoparticles, dihexadecylphosphate, and tyrosinase for the determination of catechol in natural water, Enzym. Microb. Technol. 84 (2016) 17–23.
[20] J.J. Pedrotti, L. Angnes, I.G.R. Gutz, Miniaturized reference electrodes with microporous polymer junctions, Electroanalysis 8 (1996) 673–675.
[21] R.A.B. Silva, R.H.O. Montes, E.M. Richter, R.A.A. Munoz, Rapid and selective determination of hydrogen peroxide residues in milk by batch injection analysis with amperometric detection, Food Chem. 133 (2012) 200–204.
[22] D.P. Rocha, R.M. Cardoso, T.F. Tormin, W.R. Araujo, R.A.A. Munoz, E.M. Richter, L. Angnes, Batch-injection analysis better than ever: new materials for improved electrochemical detection and on-site applications, Electroanalysis 30 (2018) 1386–1399.
[23] G. Vuković, A. Marinkovic, M. Obradovic, V. Radmilovic, M. Colic, R. Aleksic, P.S. Uskokovic, Synthesis, characterization and cytotoxicity of surface amino-functionalized water-dispersible multi-walled carbon nanotubes, Appl. Surf. Sci. 255 (2009) 8067–8075.
[24] S. Brunauer, P.H. Emmett, E. Teller, Adsorption of gases in multimolecular layers, J. Am. Chem. Soc. 60 (2) (1938) 309–319.
[25] E.P. Barrett, L.G. Joyner, P.P. Halenda, The determination of pore volume and area distributions in porous substances. I. Computations from nitrogen isotherms, J. Am. Chem. Soc. 73 (1) (1951) 373–380.
[26] F. Avilés, J.V. Cauich-Rodríguez, L. Moo-Tah, A. May-Pat, R. Vargas-Coronado, Evaluation of mild acid oxidation treatments for MWCNT functionalization, Carbon 47 (2009) 2970–2975.
[27] J. Čeponkus, A.P. Smilga, I. Rumskaitė, I. Puodžiūtė, V. Šablinskas, Infrared absorption spectroscopy of functionalized single-walled carbon nanotubes, Chemija 24 (2013) 9–19.
[28] U.J. Kim, C.A. Furtado, X. Liu, G. Chen, P.C. Eklund, Raman and IR spectroscopy of chemically processed single-walled carbon nanotubes, J. Am. Chem. Soc. 127 (2005) 15437–15445.
[29] Z. Zhao, Z. Yang, Y. Hu, J. Li, X. Fan, Multiple functionalization of multi-walled carbon nanotubes with carboxyl and amino groups, Appl. Surf. Sci. 276 (2013) 476–481.
[30] K. Wu, H. Qiu, J. Hu, N. Sun, Z. Zhu, M. Li, Z. Shi, Electrochemistry of double-wall carbon nanotubes encapsulating C_{60} and their spectral characterization, Carbon 50 (2012) 4401–4408.
[31] C. Liu, H. Chen, K. Dai, A. Xue, H. Chen, Q. Huang, Synthesis, characterization, and its photocatalytic activity of double-walled carbon nanotubes-TiO_2 hybrid, Mater. Res. Bull. 48 (2013) 1499–1505.
[32] P. Cañete-Rosales, V. Ortega, A. Álvarez-Lueje, S. Bollo, M. González, A. Ansón, M.T. Martínez, Influence of size and oxidative treatments of multi-walled carbon nanotubes on their electrocatalytic properties, Electrochim. Acta 62 (2012) 163–171.
[33] J.H. Lehman, M. Terrones, E. Mansfield, K.E. Hurst, V. Meunier, Evaluating the characteristics of multiwall carbon nanotubes, Carbon 49 (2011) 2581–2602.
[34] C. Fantini, A. Jorio, A.P. Santos, V.S.T. Peressinotto, M.A. Pimenta, Characterization of DNA-wrapped carbon nanotubes by resonance Raman and optical absorption spectroscopies, Chem. Phys. Lett. 439 (2007) 138–142.
[35] A. Kukovecz, C. Kramberger, M. Holzinger, H. Kuzmany, J. Schalko, M. Mannsberger, A. Hirsch, On the stacking behavior of functionalized single-wall carbon nanotubes, J. Phys. Chem. B 106 (2002) 6374–6380.
[36] M.T. Martinez, M.A. Callejas, A.M. Benito, M. Cochet, T. Seeger, A. Ansón, J. Schreiber, C. Gordon, C. Marhic, O. Chauvet, J.L.G. Fierro, W.K. Maser, Sensitivity of single wall carbon nanotubes to oxidative processing: structural modification, intercalation and functionalization, Carbon 41 (2003) 2247–2256.
[37] M.S. Dresselhaus, G. Dresselhaus, A. Jorio, Unusual properties and structure of carbon nanotubes, Annu. Rev. Mater. Res. 34 (2004) 247–278.
[38] J. Maultzsch, S. Reich, C. Thomsen, S. Webster, R. Czerw, D.L. Carroll, S.M.C. Vieira, P.R. Birkett, C.A. Rego, Raman characterization of boron-doped multiwalled carbon nanotubes, Appl. Phys. Lett. 81 (2002) 2647–2649.
[39] S. Kundu, Y. Wang, W. Xia, M. Muhler, Thermal stability and reducibility of oxygen-containing functional groups on multiwalled carbon nanotube surfaces: a quantitative high-resolution XPS and TPD/TPR study, J. Phys. Chem. C 112 (43) (2008) 16869–16878.
[40] M.E. Birch, T.A. Ruda-Eberenz, M. Chai, R. Andrews, R.L. Hatfield, Properties that influence the specific surface areas of carbon nanotubes and nanofibers, Ann. Occup. Hyg. 57 (9) (2013) 1148–1166.
[41] N.B. Mkhondo, T. Magadzu, Effects of different acid-treatment on the nanostructure and performance of carbon nanotubes in electrochemical hydrogen storage, Digest J. Nanomater. Biostruct. 9 (2014) 1331–1338.
[42] M.C. Paiva, W. Xu, M.F. Proença, R.M. Novais, E.L. Aegsgaard, F. Besenbacher, Unzipping of functionalized multiwall carbon nanotubes induced by STM, Nano Lett. 10 (2010) 1764–1768.
[43] Y. Pan, L. Lin, S.W. Chan, J. Zhao, Correlation between dispersion state and electrical conductivity of MWCNTs/PP composites prepared by melt blending, Composites Part A 41 (2010) 419–426.
[44] J.S. Stefano, D.P. Rocha, R.M. Dornellas, L.C. Narciso, S.R. Krzyzaniak, P.A. Mello, E. Nossol, E.M. Richter, R.A.A. Munoz, Highly sensitive amperometric detection of drugs and antioxidants on non-functionalized multi-walled carbon nanotubes: effect of metallic impurities? Electrochim. Acta 240 (2017) 80–89.
[45] R.H.O. Montes, J.S. Stefano, E.M. Richter, R.A.A. Munoz, Exploring multiwalled carbon nanotubes for naproxen detection, Electroanalysis 26 (2014) 1449–1453.
[46] M.C. Henstridge, E.J.F. Discknson, M. Aslanoglu, C. Batchelor-McAuley, R.G. Compton, Voltammetric selectivity conferred by the modification of electrodes using conductive porous layers or films: the oxidation of dopamine on glassy carbon electrodes modified with multiwalled carbon nanotubes, Sensor. Actuator. B 145 (2010) 417–427.
[47] J.S. Stefano, D.S. Cordeiro, M.C. Marra, E.M. Richter, R.A.A. Munoz, Batch-injection versus flow-injection analysis using screen-printed electrodes: determination of ciprofloxacin in pharmaceutical Formulations, Electroanalysis 28 (2) (2016) 350–357.
[48] R.M. Cardoso, R.H.O. Montes, A.P. Lima, R.M. Dornellas, E. Nossol, E.M. Richter, R.A.A. Munoz, Multi-walled carbon nanotubes: size-dependent electrochemistry of phenolic compounds, Electrochim. Acta 176 (2015) 36–43.
[49] L. Wang, Y. Zhang, Y. Du, D. Lu, Y. Zhang, C. Wang, Simultaneous determination of catechol and hydroquinone based on poly (diallyldimethylammonium chloride) functionalized graphene-modified glassy carbon electrode, J. Solid State Electrochem. 16 (2012) 1323–1331.
[50] H. Yin, Q. Zhang, Y. Zhou, Q. Ma, T. Liu, L. Zhu, Electrochemical behavior of catechol, resorcinol and hydroquinone at graphene–chitosan composite film modified glassy carbon electrode and their simultaneous determination in water samples, Electrochim. Acta 56 (2011) 2748–2753.
[51] H. Du, J. Ye, J. Zhang, X. Huang, C. Yu, A voltammetric sensor based on graphene-modified electrode for simultaneous determination of catechol and hydroquinone, J. Electroanal. Chem. 650 (2011) 209–213.
[52] F. Hu, S. Chen, C. Wang, R. Yuan, D. Yuan, C. Wang, Study on the application of reduced graphene oxide and multiwall carbon nanotubes hybrid materials for simultaneous determination of catechol hydroquinone, p-cresol and nitrite, Anal. Chim. Acta 724 (2012) 40–46.
[53] L.A. Goulart, L.H. Mascaro, GC electrode modified with carbon nanotubes and NiO for the simultaneous determination of bisphenol A, hydroquinone and catechol, Electrochim. Acta 196 (2016) 48–55.
[54] S.M. Silva, F.M. Oliveira, D.D. Justino, L.T. Kubota, A. Atanaka, F.S. Damos, R.C.S. Luz, A novel sensor based on manganese azo-macrocycle/carbon nanotubes to perform the oxidation and reduction processes of two diphenol isomers, Electroanalysis 26 (2014) 602–611.
[55] S. Jiao, M. Li, C. Wang, D. Chen, B. Fang, Fabrication of Fc-SWNTs modified glassy carbon electrode for selective and sensitive determination of dopamine in the presence of AA and UA, Electrochim. Acta 52 (2007) 5939–5944.
[56] K. Wu, J. Fei, S. Hu, Simultaneous determination of dopamine and serotonin on a glassy carbon electrode coated with a film of carbon nanotubes, Anal. Biochem. 318 (2003) 100–106.
[57] V. Vinoth, J.J. Wu, A.M. Asiri, S. Anandan, Simultaneous detection of dopamine and ascorbic acid using silicate network interlinked gold nanoparticles and multi-walled carbon nanotubes, Sensor. Actuator. B 210 (2015) 731–741.
[58] L. Yang, X. Li, Y. Xiong, X. Liu, M. Wang, S. Yan, L.A.M. Alshahrani, P. Liu, C. Zhang, The fabrication of a Co (II) complex and multi-walled carbon nanotubes modified glass carbon electrode, and its application for the determination of dopamine, J. Electroanal. Chem. 731 (2014) 14–19.
[59] A. Kutluay, M. Aslanoglu, An electrochemical sensor prepared by sonochemical onepot synthesis of multi-walled carbon nanotube-supported cobalt nanoparticles for the simultaneous determination of paracetamol and dopamine, Anal. Chim. Acta 839 (2014) 59–66.
[60] U. Yogeswaran, S.M. Chen, Multiwalled carbon nanotubes with poly(-methylene blue) composite film for the enhancement and separation of electroanalytical responses of catecholamine and ascorbic acid, Sensor. Actuator. B 130 (2008) 739–749.